ARTICLE

Reaction Mechanism of One-Step Conversion of Ethanol to 1,3-Butadiene over Zn-Y/BEA and Superior Catalysts Screening†

Shu-Xuan Dang[a], Han-Xuan Liu[a], Tao Ban[a], Xin Gao[a], Zheng-Qing Huang[a], Dong-Yuan Yang[c*], Chun-Ran Chang[a,b*]

a. Shaanxi Key Laboratory of Energy Chemical Process Intensification, School of Chemical Engineering and Technology, Xi'an Jiaotong University, Xi'an 710049, China
b. Shaanxi Key Laboratory of Low Metamorphic Coal Clean Utilization, School of Chemistry and Chemical Engineering, Yulin University, Yulin 719000, China
c. Shaanxi Yanchang Petroleum (Group) Corp. Ltd., Xi'an 710065, China

(Dated: Received on April 27, 2022; Accepted on May 3, 2022)

The one-step conversion of ethanol to 1,3-butadiene has achieved a breakthrough with the development of beta zeolite supported dual metal catalysts. However, the reaction mechanism from ethanol to butadiene is complex and has not yet been fully elucidated, and no catalyst screening effort has been done based on central metal atoms. In this work, density functional theory (DFT) calculations were employed to study the mechanism of one-step conversion of ethanol to butadiene over Zn-Y/BEA catalyst. The results show that ethanol dehydrogenation prefers to proceed on Zn site with a reaction energy of 0.77 eV in the rate-determining step, and the aldol condensation to produce butadiene prefers to proceed on Y site with a reaction energy of 0.69 eV in the rate-determining step. Based on the mechanism revealed, six elements were selected to replace Y for screening superior combination of Zn-M/BEA (M=Sn, Nb, Ta, Hf, Zr, Ti; BEA: beta polymorph A) for this reaction. As a result, Zn-Y/BEA (0.69 eV) is proven to be the most preferring catalyst compared with the other six ones, and Zn-Zr/BEA (0.85 eV), Zn-Ti/BEA (0.87 eV), and Zn-Sn/BEA (0.93 eV) can be potential candidates for the conversion of ethanol to butadiene. This work not only provides mechanistic insights into one-step catalytic conversion of ethanol to butadiene over Zn-Y/BEA catalyst but also offers more promising catalyst candidates for this reaction.

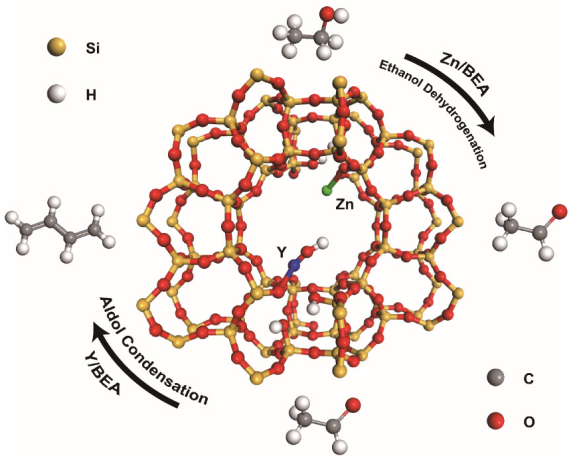

Key words: Ethanol, 1,3-Butadiene, Zn-Y/BEA, Aldol condensation, Density functional theory

I. INTRODUCTION

Nowadays, the growing tendency of C_2-C_4 olefin market is substantially expanding with their practical functionalities for the synthesis of higher value specialty chemicals [1–3]. For instance, 1,3-butadiene, an extremely important C_4 alkene platform material, has

†Part of Special Topic "the 1st Young Scientist Symposium on Computational Catalysis".
*Authors to whom correspondence should be addressed. E-mail: yangdongyuan@sxycpc.com, changcr@mail.xjtu.edu.cn

 ©2022 Chinese Physical Society

been widely used in manufacturing synthetic rubber, polymer resin, elastomer, and others [4, 5]. Hence, the preparation of butadiene is much appealing for researchers in the research area of heterogeneous catalysis [6]. Commonly, the butadiene production methods are mainly divided into three pathways, butene or butane dehydrogenation pathway, ethylene byproduct extraction pathway, and ethanol dehydrogenation pathway [7]. Detailedly, in the dehydrogenation of butene, several developed methods are available, such as the Jersey method, the Dow method, and the Shell method [8]. For the dehydrogenation of butane, there are the Houdry method and the Phillips method [9]. The synthesis methods above were initially industrialized in the 1940s and 1950s, however, the low yield of butadiene and the requirement of frequent catalyst regeneration slowed down the wide utilization of these methods. The current mainstream butadiene synthesis method with a relatively high degree of industrialization is ethylene byproduct extraction. In this way, different extractants are used to treat the C_4 distillation cut to recover butadiene. In addition, the selection of acetonitrile, dimethylformamide, and *N*-methyl pyrrolidone corresponds to the ACN method, DMF method, and NMP method, respectively [10–12]. Whereas these methods currently are facing problems such as high toxicity of the extractant, serious environmental pollution, and shortage of feed resources. By contrast, the ethanol dehydrogenation method uses ethanol as the starting material and the byproducts are mainly water and hydrogen in addition to the target product butadiene. Along with the development of bio-ethanol technology, the acquisition of ethanol is more convenient and cheaper as well, which makes the method of synthesizing butadiene from ethanol greener, more economic, and more sustainable. Due to these advantages, the ethanol conversion pathway is thought to be very hopeful for future production of butadiene.

According to different raw materials and process conditions, the ethanol dehydrogenation method is further divided into one-step method and two-step method. Specifically, the one-step method was first proposed by Lebedev [13]. In this process, ethanol is firstly dehydrogenated to form acetaldehyde, and then two molecules of acetaldehyde proceed their coupling to obtain 3-hydroxybutyraldehyde. Additionally, 3-hydroxybutyraldehyde is dehydrated to produce crotonaldehyde, which is further reduced by ethanol to obtain crotyl alcohol, and finally crotyl alcohol is dehydrated to synthesize butadiene. The two-step method refers to prepare butadiene from a mixture of ethanol and acetaldehyde, and this technology was proposed by Ostromisslensky based on the one-step method [14]. The key variation of two-step process is that the alcohol dehydrogenation and the aldehyde coupling are carried out in separate reactors with different catalysts. The two-step method has high butadiene purity, but the step-by-step reaction requires more equipment, more complicated operations, and higher cost inputs. By contrast, the one-step method requires less equipment investment and is simpler to operate, which greatly reduces production cost and has strong practical significance in the production of butadiene.

To improve the catalyst performance of one-step and two-step methods, many attempts have been made in research development of catalyst design and preparation, such as mixing binary oxide compositions of SiO_2 with MgO, ZrO_2, HfO_2, Y_2O_3 or Ta_2O_5, which have been found to be effective for C−C bond formation, and doping the oxide with d-band metals (Zn, Cu, Cr, Au, Ag) which are very effective for the conversion of ethanol to butadiene [15–23]. Currently, commonly used catalysts to produce butadiene from ethanol include molecular sieve, oxide loaded transition metal catalysts, rare earth metal catalysts, alkali metal, and alkaline earth metal catalysts, *etc.* [24–29]. Ivanova *et al.* found that hydrothermally synthesized Zr-BEA is more active than ZrO_x/SiO_2 or ZrO_x/MCM-41 catalysts, due to the higher concentration of Zr sites in Zr-BEA [30]. Dzwigaj *et al.* introduced Ta into dealuminated BEA and placed Ag, Cu and Zn dispersed nanoparticles on it and found that CuTaSi-BEA proved to be the most efficient catalyst in the one-step Lebedev process [31]. For Sn/BEA carriers, the importance of the active site environment was first suggested by Corma *et al.*, who showed that closed and open Sn sites correspond to a fully ligated Sn site (Sn-$(OSi)_4$) and a partially hydrolyzed Sn site ((HO)-Sn-$(OSi)_3$), respectively [32]. In addition, the coexistence of open and closed Zr sites in Zr-BEA was also proposed by Ivanova *et al.* that Zr open sites are more active for acetal alcohol aldol condensation [22].

In 2018, Yan *et al.* successfully produced butadiene from ethanol over a bimetallic site catalyst Zn-Y/Beta by a one-step method [33]. It was found that the C−C coupling was carried out by the condensation of two

DOI:10.1063/1674-0068/cjcp2204078 ©2022 Chinese Physical Society

molecules of acetaldehyde to give butadiene through a series of reactions and that the hydrogen removed from ethanol was used in the reduction of crotonaldehyde to crotyl alcohol. In 2020, Conrad *et al.* prepared BEA molecular sieve loaded Zn and Y bimetallic catalysts (Zn-Y/BEA) on this basis [34]. The results showed that the C−C coupling was carried out through the condensation of ethanol and acetaldehyde, which indicates that the role of ethanol in butadiene formation is not due to the transfer of hydrogen of ethanol to crotonaldehyde, but rather the involvement of ethanol in the C−C bond formation process. Although the Zn-Y/BEA catalyst has achieved high catalytic performance in the laboratory, the unclear catalyst structure and reaction mechanism lead to the inability to precisely control the process of C_2 to C_4 generation. Thus, further theoretical research is urgently needed in related fields.

In this work, we constructed a Zn-Y doped beta zeolite catalyst and conducted density functional theory (DFT) calculations to investigate the catalytic reaction mechanism and identify the active center. The microstructure of Zn-Y beta zeolite catalyst was analyzed, and the reaction mechanism of one-step production of butadiene from ethanol was clarified, including the clarification of active center, coupling method and reaction pathways. In addition, the Y atom was replaced by Sn, Nb, Ta, Hf, Zr and Ti which have been proven to be promising active sites on other supports to screen bifunctional catalysts with better catalytic performance.

II. COMPUTATIONAL DETAILS

All the DFT calculations were performed using DMol^3 code as implemented in the Materials Studio Package [35]. The generalized gradient approximation (GGA) method with Perdew-Burke-Eznzerhof (PBE) functional for the exchange-correlation term was used [36]. The double-numerical quality basis set with polarization functions (DNP) was employed. The core electrons of metal atoms were treated using effective core potential (ECP) [37]. A global real-space cutoff of 5.6 Å using fine quality setting, and a thermal smearing of 0.01 Hartree for M/BEA (M=Zn, Y, Sn, Nb, Ta, Hf, Zr, and Ti) structures were adopted. The force convergence criterion of all the structures was set to 0.002 Hartree/Å. The Brillouin zone integration was sampled using the Monkhorst-Pack scheme, and the mesh used for M/BEA was 1×1×1. The DFT-D correction was carried out by using the method of Grimme [38, 39].

The adsorption energy (E_{ads}) of an adsorbate was defined as:

$$E_{\mathrm{ads}} = E_{\mathrm{adsorbate+slab}} - E_{\mathrm{adsorbate}} - E_{\mathrm{slab}} \tag{1}$$

where $E_{\mathrm{adsorbate+slab}}$ is the total energy of the slab covered with the adsorbates, $E_{\mathrm{adsorbate}}$ is the energy of the gas-phase adsorbate, E_{slab} is the energy of the clean slab.

The reaction energy (ΔE) was calculated by the energy difference between the initial state (IS) and the corresponding final state (FS).

$$\Delta E = E_{\mathrm{FS}} - E_{\mathrm{IS}} \tag{2}$$

where E_{IS} and E_{FS} represent the energies of the IS and FS, respectively. All the discussions on energy profiles are based on approximate thermodynamics.

III. RESULTS AND DISCUSSION

A. Construction of the Zn-Y/BEA catalyst model

The catalyst models were constructed based on the zeolite Beta polymorph A (BEA), which derives from International Zeolite Association (IZA) database. The unit cell parameters are a=12.632 Å, b=12.632 Å, c=26.186 Å, $\alpha=\beta=\gamma=90°$. For the BEA structure, there is a 12-membered ring which provides an ideal channel for the catalytic reaction (FIG. 1(a)). A 13.600 Å diameter channel gives sufficient space for the process of ethanol to butadiene. We built a simplified model by keeping half of the 12-membered ring structure in the zeolite due to the big structure costing time and resource (FIG. 1(b)). The semiporous channel structure keeps only the inner two layers of atoms while H atoms are filled in the outer layer to retain the same spatial coordinates as the original atoms.

In the simplified model, one Si atom at the inner layer of channel was selected as the central atom and replaced by Zn atom or Y atom to construct Zn/BEA and Y/BEA catalyst models. Both models use open-site design, consistent with the literature report [40]. To construct Zn/BEA, we kept the other structures unchanged, and just replaced the central Si by Zn atom (FIG. 1(c)), leading to two oxygen atoms bound to Zn atom forming -Si−O−Zn−O−Si- structure and the other two oxygen atoms saturated with H forming Si−OH structures. The structure of Y/BEA

DOI:10.1063/1674-0068/cjcp2204078 ©2022 Chinese Physical Society

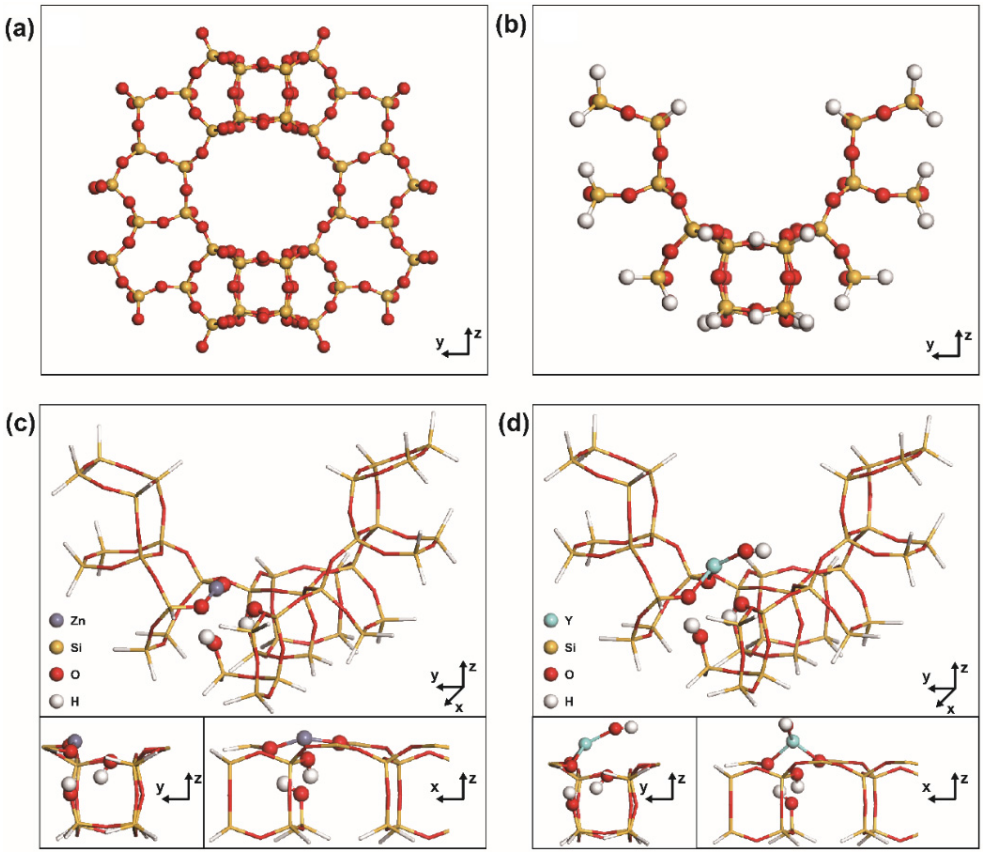

FIG. 1 Optimized structures of (a) BEA with 12-membered ring, (b) BEA with half of 12-membered ring, (c) Zn/BEA, and (d) Y/BEA.

(FIG. 1(d)) is similar to Zn/BEA, two oxygen atoms and one hydroxyl group bound to Y atom forming HO-Y-(O-Si)$_2$ structure. Both the two structures were optimized and have remarkable stability.

B. Ethanol dehydrogenation to acetaldehyde

The ethanol dehydrogenation to acetaldehyde is the first step of the reaction, which can produce the most important reactant for butadiene production. Herein, we considered the possible active sites for the ethanol dehydrogenation to acetaldehyde over Zn site and Y site. A four-step reaction pathway is carried out by DFT calculations and the energy profiles as well as the optimized structure are shown in FIG. 2. The elementary reactions are shown in Table S1 in Supplementary materials (SM). The process starts with the adsorption of ethanol on Zn or Y site. As displayed in FIG. 2(b), similar adsorption geometries of ethanol are found on both Zn and Y sites, where the hydroxyl of ethanol molecule is close to Zn or Y sites. The adsorption energies of ethanol on Zn site and Y site are −1.48 eV and −1.34 eV, respectively. These results indicate that ethanol is chemisorbed at Zn and Y sites. The next step is to break the O−H bond of ethanol and form surface ethoxide intermediates (state I to II). The dissociation of O−H is endothermic with the reaction energy of 0.30 eV and 0.81 eV on Zn site and Y site, respectively. Then the cleavage of C−H from α-H of ethanol forms H_2 with the hydrogen dissociated before (state II to III). The dissociation of C−H from α-H of ethanol is also endothermic with reaction energy of 0.77 eV and 0.42 eV on Zn site and Y site, respectively. The last step is the desorption of H_2 (state III to IV). From FIG. 2(b), we can clearly see that H_2 can be easily re-moved from the system with desorption energies of 0.21 eV for Zn/BEA and 0.07 eV for Y/BEA.

From the whole energy profiles, the rate-determining steps (RDS) of ethanol dehydrogenation to acetaldehyde on the two sites are different. On Y site, the RDS is the O−H breaking of ethanol to form the surface ethoxide intermediates (state II to III) with the reaction energy of 0.81 eV; while on Zn site, the RDS

DOI:10.1063/1674-0068/cjcp2204078 ©2022 Chinese Physical Society

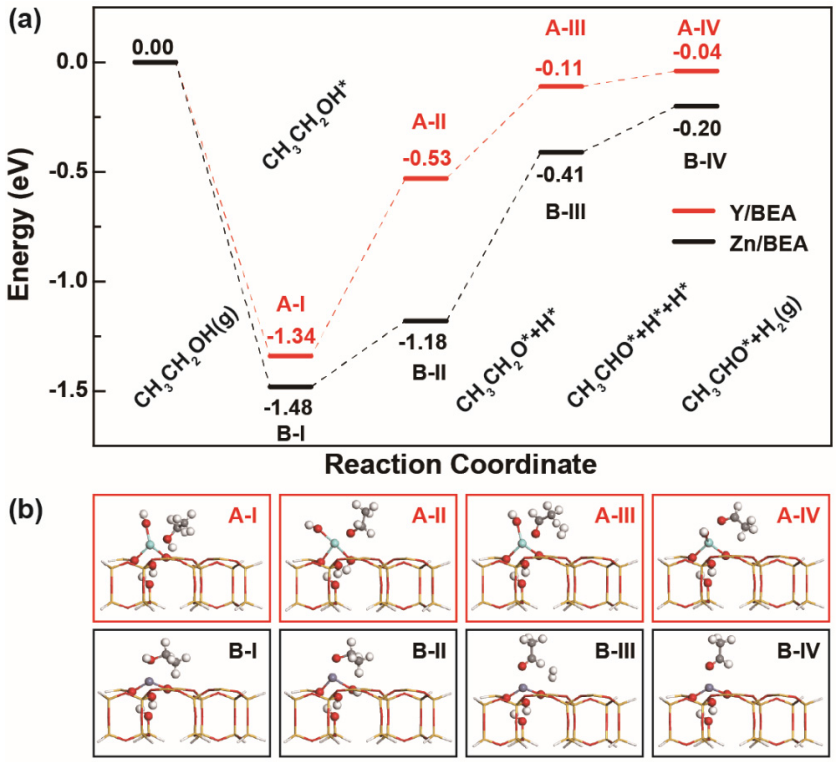

FIG. 2 (a) Energy profile of ethanol dehydrogenation on Zn/BEA (black line) and Y/BEA (red line). The zero-energy reference corresponds to the sum of CH_3CH_2OH(g) and Zn/BEA or Y/BEA. (b) Optimized structure of each step in ethanol dehydrogenation on Zn/BEA and Y/BEA.

is the C−H breaking from α-H of ethanol to form H_2 with the hydrogen dissociated before (state II to III) with the reaction energy of 0.77 eV, which is slightly lower than that on Y/BEA. Therefore, for the two active sites, Zn site shows superior performance on the ethanol dehydrogenation to acetaldehyde.

C. C−C coupling of C_2 species

For the formation of butadiene, it is important to couple C_2 species to C_4 intermediate. Thus, the aldol condensation, namely the coupling of two acetaldehyde, is significant for the process and the coupling of two acetaldehyde molecules to crotonaldehyde (the main precursor of butadiene [41]) is the focus of this work.

To understand the coupling process of C_2 species on heterogeneous catalytic site, the electronic structure analysis for the co-adsorption of acetaldehyde and derivative species is conducted by using Fukui function. Fukui function is generally used to describe the chemical reactivity by the determination of electrophilic and nucleophilic sites, and provides quantitative description with function marked as f^- and f^+ for electrophilic attack and nucleophilic attack, respectively. For showing

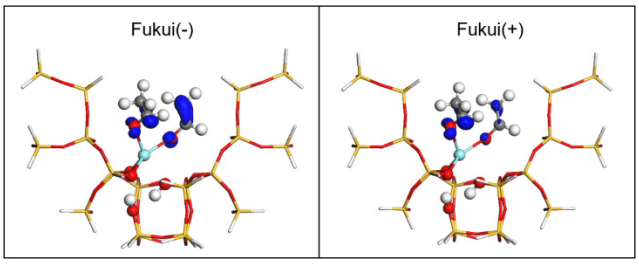

FIG. 3 Isosurface of Fukui function upon the adsorption of acetaldehyde and enolate intermediate on Y/BEA.

the reactivity of sites visualized, dual descriptor f^2 as a numerical descriptor of atoms is calculated from the results of Fukui function. The absolute value of f^2 is positively correlated with the reaction activity, and the reaction between atoms with positive and negative extremum of f^2 will occur easily. The isosurface of Fukui function is shown in FIG. 3, where one of the acetaldehyde is transformed into enolate intermediate through the keto-enol tautomerism. According to the result (Table S2 in SM), the f^+ and f^- both show the α-C as reactive site of acetaldehyde. The value of f^2 for the α-C site is 0.06, which means this carbon atom is an

DOI:10.1063/1674-0068/cjcp2204078 ©2022 Chinese Physical Society

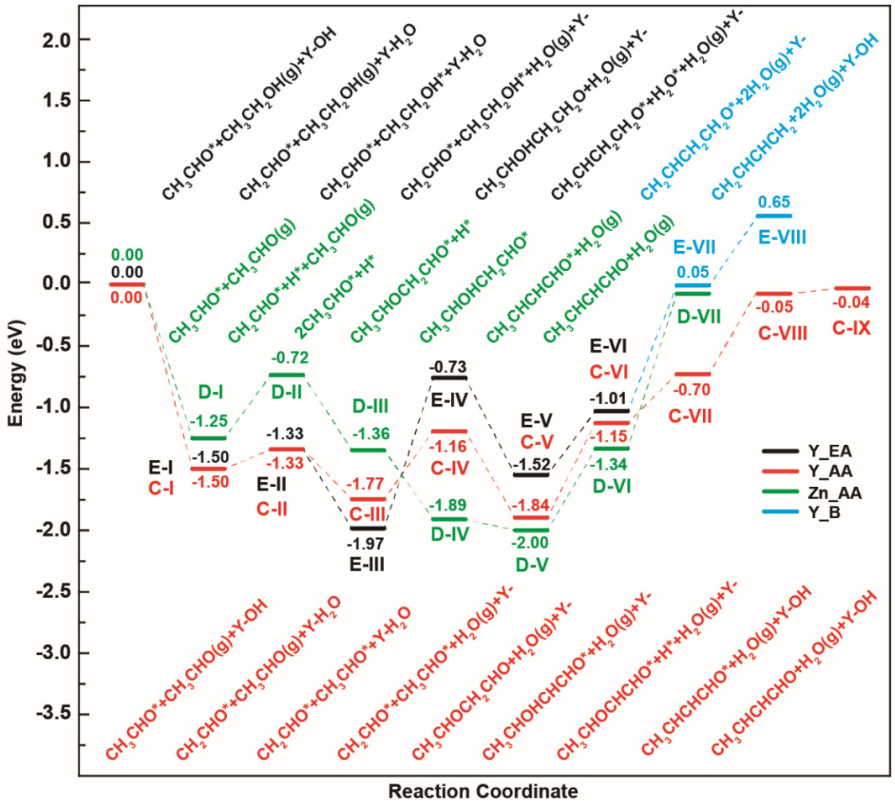

FIG. 4 Energy profiles of differnent reaction pathways. Green and red lines represent the aldol condenstaion on Zn site and Y site, respectively; black line represents the condenstaion between acetaldehyde and ethanol on Y site; cyan line represents the formation of butadiene.

electrophilic site, and the superposition of the results of f^+ and f^- means the absence of an appropriate nucleophilic site. The coupling between two electrophilic sites will be difficult, and thus the direct coupling between acetaldehyde molecules is unlikely to occur. However, for the enolate intermediate, the f^- shows an obvious value on β-C site. The value of f^2 for the site is -0.034, which suggests that this β-C site can be a suitable nucleophilic site. Thus, the coupling reaction that the β-C of the enolate structure acts as a nucleophile to attack the α-C of acetaldehyde is expectable. It is worth noting that the value of f^+ for enolate intermediate is weak, indicating that electrophilic site in enolate is lacking and the coupling between two enolate intermediates is difficult too. The results of Fukui function verify the feasibility of C−C coupling and suggest that the transformation of one acetaldehyde to enolate intermediate is necessary.

Based on the analysis above, two aldol condenstaion pathways marked as Y_AA and Zn_AA are carried out depending on the active site. The thermodynamic calculation results and optimized structures of each step are shown in FIG. 4 and FIG. 5, respectively. And the elementary reactions are shown in Table S3 in SM. On both the Zn site and the Y site, the first acetaldehyde molecule is transformed into enolate intermediate for the following coupling reaction. On the Zn site, the α-H of acetaldehyde is easy to be abstracted by the surface oxygen site and the acetaldehyde is transformed into an enolate intermediate (D-II). Then the second acetaldehyde molecule adsorbs on the Zn site to couple with the enolate group. Afterwards, the H atom returns from O site on the surface to the coupled C_4 species and forms the classic aldol structure with an exothermic reaction energy of 0.11 eV. At last, the aldol molecule dehydrates and forms crotonaldehyde. It is worth noting that the crotonaldehyde product is strongly adsorbed on the Zn site with the adsorption energy of 1.29 eV, and the step of desorption is the rate-determining step of the process on Zn site.

Another aspect is the aldol condensation on Y site. Different from the process on Zn site, the hydroxyl group on Y site can play a unique role and change the reaction pathway. In the ethanol dehydrogenation stage,

DOI:10.1063/1674-0068/cjcp2204078 ©2022 Chinese Physical Society

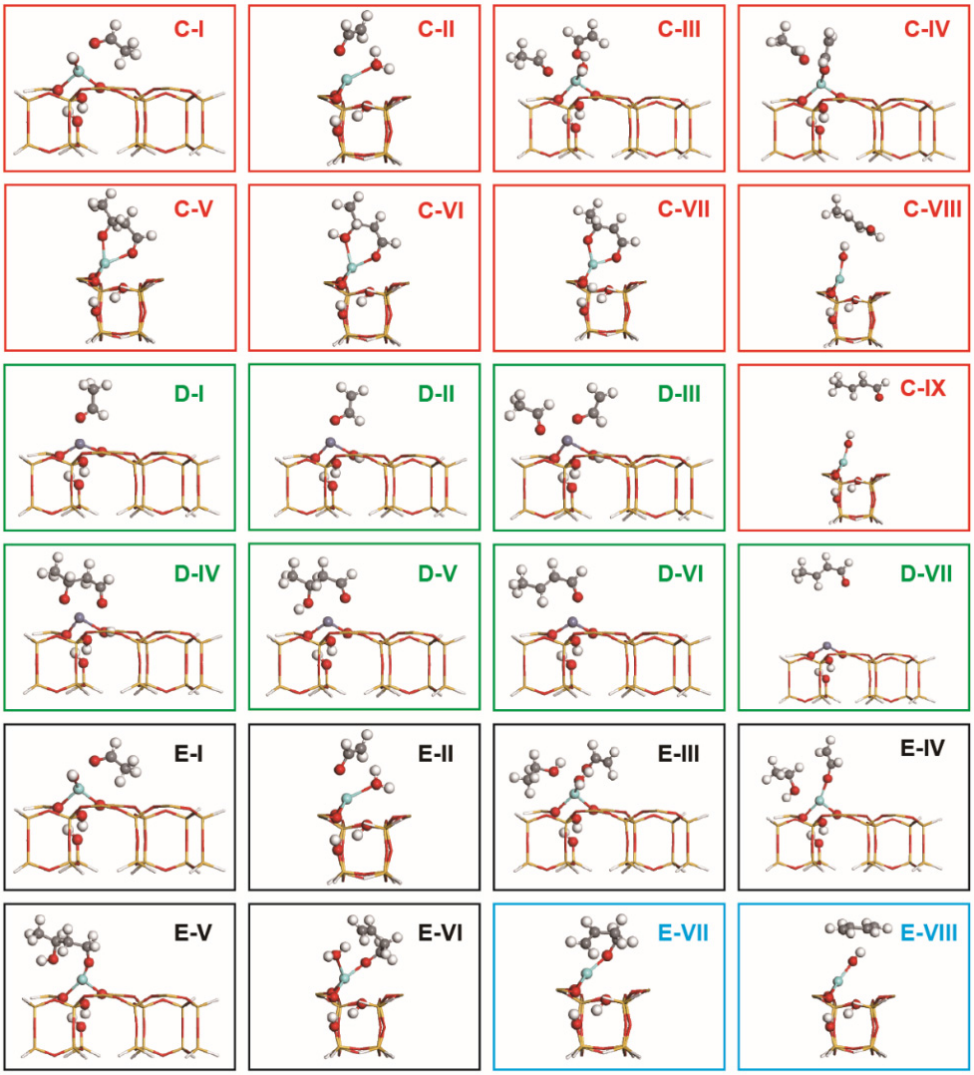

FIG. 5 Optimized structures of the intermediates labeled in FIG. 4.

we have found that the combination of dissociated protons with Y−O site will repel the Y−OH structure and cause a relatively high reaction energy. Therefore, we assume that the dissociated protons might be transferred to Y−OH in the form of adsorbed water. In this way, not only the problem of steric confinement is solved, but also the dehydration step in the reaction process is simplified by the removal and recovery of the Y−OH structure. After the introduction of the second acetaldehyde, the adsorption of H_2O is weakened and desorbs facilely to the gas-phase with the de-sorption energy of 0.61 eV. Then the adsorbed acetaldehyde will couple with the enolization intermediate of the first acetaldehyde to obtain the C_4 intermediate CH_3CHOCH_2CHO, which combines with the Y atom via a stable hexacyclic structure. The process of dehydration directly before co-adsorption is also considered, but its results are not as favorable as co-adsorption first and then dehydration, as shown in FIG. S1 in SM. After the coupling, the hydrogen which used to be α-H of the first acetaldehyde will transfer to oxygen atom on the Y−O−Si structure and form $CH_3CHOCHCHO$, then the C−O bond of the $CH_3CHOCHCHO$ breaks to form $CH_3CHCH{-}CHO$. Similarly, the hydrogen on Y−O−Si will transfer to the oxygen attached to Y site to recover the Y−OH structure and obtain crotonaldehyde. With the steric hindrance of hydroxyl group, the desorption energy of crotonaldehyde on Y site is much lower than that on Zn site, and the rate-determining step is the dehydrogenation of CH_3CHOCH_2CHO with

DOI:10.1063/1674-0068/cjcp2204078 ©2022 Chinese Physical Society

energy change of 0.69 eV. Because the Si−OH groups are not exposed to the channel, the H-transfer to Si−OH is hence not considered.

By comparing the overall energy profile, the Y site presents the better performance than Zn site in the C−C coupling to form crotonaldehyde. Comparing the rate-determining step, the most difficult step on Zn_AA is endothermic by 1.29 eV, which is remarkably higher than that on Y_AA. The hydroxyl group connected with Y site plays a positive role in the desorption of product and changes the rate-determining step. Noting that Y−OH group participates in the elementary steps as a water formation promoter and a H-transfer mediator, which shows low reaction energy in most cases and also provides more potential advantage of reaction kinetics than Zn site. These results indicate that the aldol condensation process tends to react on Y site.

D. Butadiene formation

Based on crotonaldehyde generated above, butadiene can be formed via Meerwein-Ponndorf-Verley (MPV) reduction of crotonaldehyde and dehydration steps as shown in the Y_B pathway in FIG. 4. This process can occur on acid sites of zeolite, and plenty of the work has been done. Thus, this classic multistep mechanism will not be repeated in this work. In addition, butadiene could also be produced directly from the condensation of ethanol and acetaldehyde as depicted by the Y_EA pathway in FIG. 4. The adsorption and enolization of acetaldehyde follow the same mechanism as the above-mentioned Y_AA pathway. Subsequently, ethanol is introduced and couples with the enolization intermediate to obtain C_4 intermediate, accompanied with the α-H of ethanol transfer to the α-C of enolization intermediate forming the $CH_3CH(OH)CH_2CH_2O^*$. Then the hydroxyl group transforms to the Y site for re-generating the structure of Y−OH and conducts the dehydration step to form $CH_2{=}CHCH_2CH_2O^*$ species. After the proton transfer with the help of Y−OH group, the target product butadiene forms and desorbs into the gas-phase. This pathway shows the energy change of the rate-determining step as 1.24 eV, which is less favorable than the formation of butadiene via crotonaldehyde. Therefore, the aldol condensation followed by MPV reduction on Y site is considered as the main pathway for the production of butadiene.

E. Catalytic cycle

To sum up the above, the synthesis of butadiene over Zn-Y/BEA catalysts is the combination of the ethanol dehydrogenation cycle over Zn site and the condensation cycle of two acetaldehydes over Y site. The whole reaction mechanism is shown in FIG. 6. Ethanol first adsorbs on the Zn site. The dehydrogenation step is completed by two-step proton transfer to generate acetaldehyde and H_2. The acetaldehyde desorbs from the Zn site to the Y site and starts the cycle of aldol condensation. The first molecule of acetaldehyde undergoes enolization to obtain an enolized intermediate. The dissociated β-H will form water with the hydroxyl group on the Y site and be removed. After the second molecule of acetaldehyde adsorbs on the Y site, the C of the enolate intermediate acts as a nucleophile to attack the carbonyl carbon in the second molecule of acetaldehyde. Thus, the C_4 intermediate CH_3CHOCH_2CHO can be obtained and transforms to crotonaldehyde by two steps of proton transfer. In the whole condensation cycle, Y−OH is involved in the reaction. Finally, crotonaldehyde is reduced by MPV reaction with H_2 on the acid sites of zeolite and the target product is obtained to be butadiene through proton transfer.

F. Superior catalysts screening

The results above have clearly shown that the type of central metal atoms can affect the activity of the catalyst. We thus try to replace the central metal atoms for screening superior catalysts for this reaction. Because the aldol condensation is determinative to the formation of butadiene, thus only the replacement of Y by Ti, Zr, Hf, Sn, Nb, and Ta atoms is considered. The selected metals are in the same group or in the neighboring group with Y atom in the periodic table. Among them, Nb, Ta, and Ti adopt the same three-coordination structure as Y (FIG. S2 in SM). While Sn, Hf, and Zr adopt four-coordination structures as shown in FIG. S3 in SM. All the structures are used to investigate aldol condensation process beginning with two adsorbed acetaldehyde molecules, consistent with the Y_AA route. The reaction energies of the elementary steps involved in this reaction on M/BEA catalysts are shown in FIG. 7.

From FIG. 7, one can see that the adsorption of acetaldehyde on Ta is the strongest (−2.15 and −1.92 eV for first and second acetaldehyde adsorption, respectively) compared to other catalysts, while the ad-

DOI:10.1063/1674-0068/cjcp2204078 ©2022 Chinese Physical Society

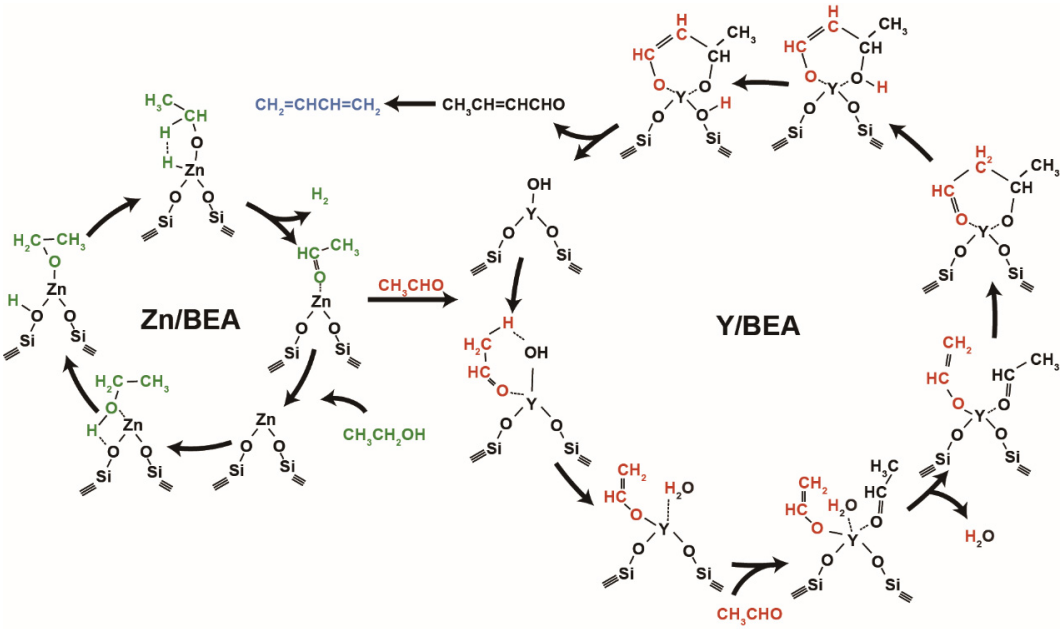

FIG. 6 Schematic diagram of the mechanism of butadiene formation from ethanol over Zn-Y/BEA catalyst.

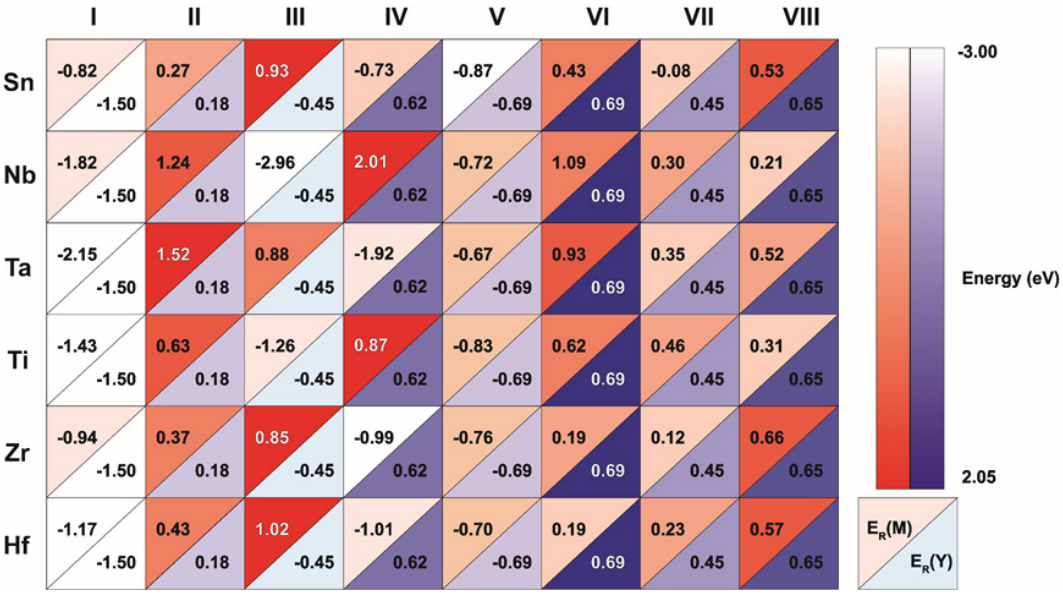

FIG. 7 Reaction energy of aldol condensation on M/BEA (M=Sn, Nb, Ta, Ti, Zr, Hf).

sorption of acetaldehyde on Sn is weaker (−0.82 and −0.73 eV for first and second acetaldehyde adsorption, respectively) than others. This is consistent with the volcano curve, that too strong adsorption or too weak adsorption is not conducive to the progress of the catalytic reaction. Besides, we find an interesting phenomenon related to the coordination environment of central atom. Specially, just Ti site could adsorb three molecules at same time as Y site, thus the desorption of water is prior to the introduction of the second acetaldehyde molecule on other metal sites. As shown in FIG. 7, the central atom with three-coordination structure, such as Ta/BEA, Nb/BEA, and Ti/BEA, has a lower relative energy in steps like adsorption and aldol condensation. This led to a higher reaction energy of next reaction steps. While the situation on the central atom with four-coordination structure, such as Sn/BEA, Hf/BEA, and Zr/BEA, is dramatically differ-

DOI:10.1063/1674-0068/cjcp2204078 ©2022 Chinese Physical Society

ent. The central atom with four-coordination structure has better performance in aldol condensation reaction. Thus, we find that the central doping atom is not the only factor affecting reactivity. The coordination environment of the central atom also has considerable impact on the reactivity.

Among these catalysts, the rate-determining steps of the whole aldol condensation pathway on the seven catalysts are different. On Sn/BEA (0.93 eV), Zr/BEA (0.85 eV), Hf/BEA (1.02 eV), and Ti/BEA (0.87 eV). The rate-determining step are the removing hydroxyl group on M with the formation of water (state II to III), where the value in the parentheses denotes the reaction energy of the RDS. On Nb/BEA (1.39 eV), the rate-determining step is the transfer of protons (state V to VI), while on Ta/BEA (1.52 eV), the rate-determining step is the enolization step (state I to II). Comparing the rate-determining steps on these M/BEA catalysts, one can see that most of the M/BEA catalysts have a lower rate-determining step. But Y/BEA is still the most ideal one with the reaction energy of the RDS being 0.69 eV. Zr/BEA, Ti/BEA, and Sn/BEA also show the rate-determining reaction energy lower than 1 eV, which can be the potential candidates for the reaction of aldol condensation.

IV. CONCLUSION

In summary, we have thoroughly investigated the reaction mechanisms of the conversion of ethanol to butadiene over Zn-Y/BEA catalyst by DFT calculations. Based on our results, the reaction pathways can be divided into three stages that are the ethanol dehydrogenation to acetaldehyde, the aldol condensation of acetaldehyde to crotonaldehyde, and the crotonaldehyde reduction to butadiene. The ethanol dehydrogenation is found to preferentially occur on Zn site rather than Y site. While the aldol condensation is found to preferentially occur on Y site rather than Zn site because of the involvement of the special Y−OH structure. On the basis of the reaction mechanisms revealed, six more elements (Sn, Nb, Ta, Hf, Zr, Ti) are selected to replace Y for searching superior catalysts for the aldol condensation step. It turns out that Y/BEA is still the most preferrable catalyst with the lowest reaction energy of rate-determining step (0.69 eV), while Zr/BEA (0.85 eV), Ti/BEA (0.87 eV) and Sn/BEA (0.93 eV) can also be potential candidates for the reaction of aldol condensation. This work not only provides a profound understanding on the catalytic conversion of ethanol to butadiene over Zn-Y doped zeolite catalyst but also suggests more promising catalyst candidates for the one-step conversion of ethanol to butadiene.

Supplementary materials: Elementary reactions of ethanol dehydrogenation to acetaldehyde, Fukui index of selected sites, elementary reactions of acetaldehyde condensation, elementary reactions of ethanol-acetaldehyde condensation, reaction energy profiles and optimized structures are shown.

V. ACKNOWLEDGMENTS

This work was supported by the National Natural Science Foundation of China (No.22078257, No.22038011, and No.22108213), the National Key R&D Program of China (No.2020YFA0710000), the China Postdoctoral Science Foundation (No.2018T111034 and No.2021M692548), and the Rising Star Program in Science and Technology of Shaanxi Province (No.2020KJXX-079). Chun-Ran Chang also acknowledges the support from the K. C. Wong Education Foundation. The calculations were performed by using the HPC Platform at Xi'an Jiaotong University.

[1] C. Angelici, B. M. Weckhuysen, and P. C. A. Bruijnincx, ChemSusChem **6**, 1595 (2013).
[2] G. Pomalaza, P. A. Ponton, M. Capron, and F. Dumeignil, Catal. Sci. Technol. **10**, 4860 (2020).
[3] E. V. Makshina, M. Dusselier, W. Janssens, J. Degreve, P. A. Jacobs, and B. F. Sels, Chem. Soc. Rev. **43**, 7917 (2014).
[4] I. Bin Samsudin, H. Zhang, S. Jaenicke, and G. K. Chuah, Chem-Asian J. **15**, 4199 (2020).
[5] G. Pomalaza, M. Capron, V. Ordomsky, and F. Dumeignil, Catalysts **6**, 203 (2016).
[6] P. I. Kyriienko, O. V. Larina, S. O. Soloviev, and S. M. Orlyk, Theor. Exp. Chem. **56**, 213 (2020).
[7] D. Cespi, F. Passarini, I. Vassura, and F. Cavani. Green Chem. **18**, 1625 (2016).
[8] B. Z. Qian and X. H. Li, Chem. Ind. **33**, 33 (2015).
[9] J. Lu, *Master of Engineering, Dissertation*, Tianjin: Tianjin University, (2018).
[10] H. Chang and P. Liang, Refin. Chem. Ind. **19**, 34 (2008).
[11] Z. Lei, R. Zhou, and Z. Duan, Chem. Eng. J. **85**, 379 (2002).
[12] C. Niu, Petrochem. Ind. Technol. **15**, 39 (2008).
[13] S. Lebedev, Zh Obshch Khim. **3**, 698 (1933).

DOI:10.1063/1674-0068/cjcp2204078 ©2022 Chinese Physical Society

[14] J. Ostromislenskiy, J. Russ. Phys. Chem. Soc. **47**, 1472 (1915).
[15] Q. Zhu, B. Wang, and T. Tan, ACS Sustain. Chem. Eng. **5**, 722 (2017).
[16] M. Zhang, J. Zhuang, and Y. Yu. Appl. Surf. Sci. **458**, 1026 (2018).
[17] A. Miyaji, M. Hiza, Y. Sekiguchi, S. Akiyama, A. Shiga, and T. Baba, J. Jpn. Pet. Inst. **61**, 171 (2018).
[18] W. Reschetilowski, M. Hauser, F. Alscher, M. Klauck, and G. Kalies, Catalysts **10**, 854 (2020).
[19] C. Angelici, M. E. Z. Velthoen, B. M. Weckhuysen, and P. C. A. Bruijnincx, Catal. Sci. Technol. **5**, 2869 (2015).
[20] P. Muller, S. P. Burt, A. M. Love, W. P. McDermott, P. Wolf, and I. Hermans, ACS Catal. **6**, 6823 (2016).
[21] G. M. C. Gonzalez, A. L. V. Perales, A. Martinez, M. Campoy, and F. Vidal-Barrero, Fuel Process. Technol. **226**, 107092 (2022).
[22] V. L. Sushkevich and I. I. Ivanova, ChemSusChem **9**, 2216 (2016).
[23] X. Dong, C. Liu, D. Fan, Y. Yu, and M. Zhang, Appl. Surf. Sci. **481**, 576 (2019).
[24] S. Kvisle, A. Aguero, and R. P. A. Sneeden, Appl. Catal. **43**, 117 (1988).
[25] O. V. Larina, N. D. Shcherban, P. I. Kyriienko, I. M. Remezovskyi, P. S. Yaremov, I. Khalakhan, G. Mali, S. O. Soloviev, S. M. Orlyk, and S. Dzwigaj, ACS Sustain. Chem. Eng. **8**, 16600 (2020).
[26] G. Yang, E. A. Pidko, and E. J. M. Hensen, J. Phys. Chem. C. **117**, 3976 (2013).
[27] B. D. Montejo-Valencia, J. L. Salcedo-Pérez, and M. C. Curet-Arana, J. Phys. Chem. C **120**, 2176 (2016).
[28] B. D. Montejo-Valencia, Y. J. Pagán-Torres, M. M. Martínez-Iñesta, and M. C. Curet-Arana, ACS Catal. **7**, 6719 (2017).
[29] W. Dai, S. Zhang, Z. Yu, T. Yan, G. Wu, N. Guan, and L. Li. ACS Catal. **7**, 3703 (2017).
[30] V. L. Sushkevich, I. I. Ivanova, and E. Taarning, Green Chem. **17**, 2552 (2015).
[31] P. I. Kyriienko, O. V. Larina, S. O. Soloviev, S. M. Orlyk, C. Calers, and S. Dzwigaj, ACS Sustain. Chem. Eng. **5**, 2075 (2017).
[32] M. Boronat, P. Concepcion, A. Corma, M. Renz, and S. Valencia, J. Catal. **234**, 111 (2005).
[33] T. Yan, W. Dai, G. Wu, S. Lang, M. Hunger, N. Guan, and L. Li, ACS Catal. **8**, 2760 (2018).
[34] L. Qi, Y. Zhang, M. A. Conrad, C. K. Russell, J. Miller, and A. T. Bell, J. Am. Chem. Soc. **142**, 14674 (2020).
[35] B. Delley, J. Chem. Phys. **113**, 7756 (2000).
[36] J. P. Perdew, K. Burke, and M. Ernzerhof, Phys. Rev. Lett. **77**, 3865 (1996).
[37] A. Bergner, M. Dolg, W. Kchle, H. Stoll, and H. Preuß, Mol. Phys. **80**, 1431 (2006).
[38] S. Grimme, J. Comput. Chem. **27**, 1787 (2006).
[39] S. Grimme, WIREs Comput. Mol. Sci. **1**, 211 (2011).
[40] M. Zhang, X. Guan, J. Zhuang, and Y. Yu, Appl. Surf. Sci. **579**, 152212 (2022).
[41] J. Zhang, E. C. Wegener, N. R. Samad, J. W. Harris, K. A. Unocic, L. F. Allard, S. Purdy, S. Adhikari, M. J. Cordon, J. T. Miller, T. R. Krause, S. Cheng, D. Liu, M. Li, X. Jiang, Z. Wu, and Z. Li, ACS Catal. **11**, 9885 (2011).

DOI:10.1063/1674-0068/cjcp2204078 ©2022 Chinese Physical Society